LEAST SQUARES IDENTIFICATION WITH APPLICATION TO SHAPE CONTROL

IN A SENDZIMIR COLD ROLLING STEEL MILL

J.V. Ringwood

. School of Electronic Engineering
National Institute for Higher Education
Glasnevin, Dublin 9, Republic of Ireland

ABSTRACT

A least squares technique for the on-line identification of the input/output characteristics of a Sendzimir rolling cluster is presented. Based on this technique, explicit and implicit self-tuning shape control schemes, using existing control algorithms, are derived. Two control structures, utilising different numbers of plant control inputs, are considered. While a simplistic approach to the problem is taken (resulting in easily implementable self-tuning schemes), the parameter estimates and subsequent control achieved are shown to be adequate for the application. A variety of simulation results are given.

1. INTRODUCTION

In the last decade, a substantial amount of work has been undertaken in the development of an automatic shape control system for a Sendzimir mill (1-5). By shape control is meant the control of internal stresses in the strip such that it does not buckle when cut into small sections (not to be confused with gauge control). Much of the work carried out in this area has been concerned with modelling the mill in both its static (involving the rolling cluster) and dynamic (involving the actuators, strip dynamics and shapemeter) parts. Rolling cluster models have been developed independently by Gunawardene (1) and Dutton (2) and are assumed to be independent of frequency i.e. a step change in the position of the actuators produces an instantaneous change in roll-gap shape profile. However, the linearised gain matrices produced by each model, for similar mill conditions, do not agree (though they are of the same order of magnitude) and neither model has been conclusively validated by plant tests (due to the large expense involved). Furthermore, the gains relating shape profile changes to changes in actuator positin are nonlinear , the gains varying with actuator position.

The control schemes developed utilise the As-U-Rolls (AUR's) only (3-5) (currently being commissioned) or both AUR's and first intermediate rolls (FIR's)(6). The location of these shape control devices is shown in Fig.2. All of the control algorithms rely heavily on the AUR or both AUR and FIR mill matrices, and while a good degree of robustness for these controllers has been demonstrated (5),(6), performance degradation will occur for an inaccurate controller. Another source of inaccuracy is the plant/controller mismatch resulting from the use of a controller for a schedule (or pass) other than the one for which it was designed. This mismatch arises from the need to economise in the number of controllers required to be stored to cover all schedules and passes (over 3000 different schedules exist). Each schedule demands particular mill conditions (roll diameters, etc.) resulting in different gain matrices for each schedule. Due to the heavy computational effort involved in the gain calculations, evaluation of the mill matrices must be performed off-line and the results stored for subsequent use. The problems of plant/controller mismatch for this variety of reasons may be alleviated by the use of a self-tuning control algorithm incorporating identification of the relevant mill matrices. Such a scheme would produce the correct controller for each pass of each schedule, and furthermore track the mill gains which change with actuator positions.

2. SENDZIMIR MILL MODEL

A view of the physical layout of the mill, showing its relevant component parts, is given in Fig.2. A block diagram of the mill model (and associated controllers) is shown in Fig.1. All the interaction between paths takes place in the rolling cluster, represented by the mill gain matrices $G_a \in R^{8 \times 2}$ and $G_i \in R^{8 \times 2}$ for the AUR's and FIR's respectively. The dynamic actuator blocks consist of position control loops (shown in Fig.3), the parameter values differing slightly between the AUR and FIR cases, given as:

	k_c	δ_1 (mm)	τ (secs)	k_i (mm/s)	δ_2 (mm)
AUR	1.3	0.5	0.05	8.0	0.3
FIR	0.7	0.5	0.1	3.13	0.5

g(s) accounts for the strip and shapemeter dynamics and has the form:

$$g(s) = \frac{e^{-\tau_1 s}}{(1 + \tau_2 s)(1 + \tau_3 s)}$$

the values of τ_1, τ_2 and τ_3 for different strip speeds given from the following table:

v(m/s)	2	5	15
τ_1(secs)	1.455	0.582	0.194
τ_2(secs)	2.66	1.064	0.354
τ_3(secs)	1.43	0.74	0.3

The shape profile is modelled as an eight point profile, the input and output shape profiles therefore being represented by eight variables. The input shape profile is considered as a disturbance to the system and is assumed to consist of a constant profile with small amplitude sinusoidal variations in each profile point. The other disturbance to the system is the measurement noise on the shapemeter. It consists of two sinusoidal components, one dependent on strip speed and the other independent. A full description of these disturbances is given in (6).

3. CONTROL STRATEGIES

Control algorithms have been developed to control the AUR's only (scheme currently being commissioned)(3) and, more recently, to control both AUR's and FIR's (6). The structure of each of these control systems is shown in Fig.1.

3.1 As-U-Roll Control System

In this control system, the position of the FIR's are set manually, automatic shape control being provided only via the AUR's. Since all the interaction in the relevant part of the model occurs in the AUR mill matrix, it is reasonable to attempt to diagonalise the system by the inclusion of an inverse of G_a in K and designing the resulting single loops via $k_1(s)$. However, due to certain symmetry properties (1), G_a is singular and cannot be inverted directly. Application of the transformation matrices
$$P \in R^{4 \times 8} \quad \text{and} \quad P^T \in R^{8 \times 4}$$
yield a reduced mill matrix $G_x \in R^{4 \times 4}$ which is invertible, where:

$$G_x = PG_aP^T \qquad (1)$$

K may now be chosen as G_x^{-1}, that is:

$$K = (PG_aP^T)^{-1} \qquad (2)$$

P contains the $1^{st} \to 4^{th}$ order Gram polynomials, so control is applied only to the first to fourth order components in the shape profile. This, however, is adequate for the application. For a medium speed plant (5 m/s) $k_1(s)$ is chosen as:

$$k_1(s) = \frac{300(1 + 1.428s)}{(1 + 1000s)} \qquad (3)$$

3.2 Combined AUR/FIR Control System

In this scheme, both AUR's and FIR's are utilised to provide automatic shape control giving greater range of, and more powerful control of, strip shape. A similar approach to that taken in 3.1 is used, in that control is exerted on a "parameterised" shape profile and an attempt is made to diagonalise the system using a constant precompensator, in this case $N \in R^{6 \times 4}$. For this configuration, however, it is first necessary to "equalise" the AUR and FIR actuators using c_a and c_i so that

$$f_a c_a = f_i c_i = h(s) \qquad (4)$$

where h(s) is a constant transfer function. (7) describes a method for the calculation of $c_a(s)$ and $c_i(s)$. The plant, with the addition of the transformations and equalising compensators, becomes:

$$W(s) = [PG_aP^T \quad PG_i] \, g(s)h(s) \qquad (5)$$

N may now be chosen so that

$$[PG_aP^T \quad PG_i] \, N = I_4 \qquad (6)$$

and $k_2(s)$ chosen to compensate $g(s)h(s)$. For a medium (5 m/s) speed plant, $k_2(s)$ is chosen as

$$k_2(s) = \frac{200 \, (2.0s + 1)}{(1000s + 1)(0.9s + 1)} \qquad (7)$$

Note that N, defined in (6) is, in general, not unique. It may, however, be chosen uniquely via the Moore-Penrose inverse (8), (denoted by N^*) as:

$$N^* = A^T(AA^T)^{-1} \qquad (8)$$

where

$$A = [PG_aP^T \quad PG_i] \qquad (9)$$

4. PARAMETER ESTIMATION

It is seen from (2) and (6) that K and N are highly dependent on G_a and G_i. It is therefore desireable that good estimates of G_a and G_i are available over the complete range of mill operation. If the mill matrices can be estimated on-line, then the controller matrices K and N may be calculated, resulting in explicit self-tuning schemes. Alternatively it may be possible to estimate K and N directly, resulting in implicit schemes. Since it is required to estimate the mill matrices, measurements of output and input signals as close as possible to the rolling cluster are desireable. The rolling cluster positions are measureable directly, being the actuator positions (shown as u_a" and u_i" in Fig.1). The nearest available outputs, however, are the shapemeter measurements (shown as y in Fig.1). Since it is only required to estimate the reduced mill matrices (see equations (1) and (9)), the transformed output y_p may be used for estimation purposes.

4.1 As-U-Roll Scheme

The equation relating y_p to u_a" is given by:

$$y_p = PG_a \, g(s) \, u_a" \qquad (10)$$

ignoring incoming strip shape and measurement disturbances. Define:

$$u_a' = P \, u_a" \qquad (11)$$

giving

$$u_a" = P^T \, u_a'$$

since $P^TP = I$ (orthonormal polynomials), and define:

$$u_a = g(s) \, u_a' \qquad (12)$$

(obtained by passing u_a' through a simulated transfer function g(s)). Equation (10) may now be rewritten as:

$$y_p = PG_aP^T \, u_a = G_x \, u_a \qquad (13)$$

which is in a form suitable for the identif-

ication of PG_aP^T. Writing out (13) in elemental form gives:

$$y_i = \sum_{j=1}^{4} g_{ij}u_j , \quad 1 \le i \le 4 \qquad (14)$$

where g_{ij} are the elements of G_x, and

$$Y_p = (y_1 \ y_2 \ y_3 \ y_4)^T , \quad u_a = (u_1 \ u_2 \ u_3 \ u_4)^T$$

or
$$y_i = g_i^T u_a \qquad (15)$$
where
$$g_i^T = (g_{i1} \ g_{i2} \ g_{i3} \ g_{i4})$$

Assuming a series of observations $y_i(1), y_i(2)$ ... and $u_a(1), u_a(2),...$ are available, the least squares estimate of row i of G_x which minimises the cost criterion

$$J(g_i) = (Y_i - g_i^T U)^T (Y_i - g_i^T U) \qquad (16)$$

is given as:

$$g_i^T = Y_i U^T (UU^T)^{-1} \qquad (17)$$

where
$$Y_i = (y_i(1) \ y_i(2) \ ....)$$
and
$$U = (u_a(1) \ u_a(2) \ ....)$$

Note that at least four corresponding measurements of y_i and u_a are required before the matrix (UU^T) in (17) is rendered invertible. The calculation in (17) must be performed four times (i = 1,4) to get estimates for all the rows of G_x. The estimation of G_x using (17) requires a relatively large amount of data to be stored. In addition, a continuous updating of the estimates is difficult to perform. A recursive set of equations, more suitable for the on-line identification of G_x are given (6), (9) as:

$$R(k+1) = R(k) - R(k)u_a(k+1)[1+u_a^T(k+1)R(k)u_a(k+1)]^{-1}$$
$$.u_a^T(k+1)R(k) \qquad (18)$$

and
$$\hat{g}_i^T(k+1) = \hat{g}_i^T(k) + \{y_i(k+1) - \hat{g}_i^T(k)u_a(k+1)\}$$
$$.u_a^T(k+1)R(k+1) \qquad (19)$$

where $R \in R^{4 \times 4}$ is the error covariance matrix. Note that the 4x4 matrix inversion in (17) has been reduced to the scalar inversion in (18). Using the estimate of G_x from (18) and (19), K may be evaluated via (2) giving explicit self-tuning control. However, (13) may be rearranged to give:

$$u_a = G_x^{-1} Y_p \qquad (20)$$

and a recursive least squares estimate for the rows of G_x^{-1} obtained via:

$$R(k+1) = R(k) - R(k)y_p(k+1)[1+y_p^T(k+1)R(k)y(k+1)]^{-1}$$
$$.y_p^T(k+1)R(k) \qquad (21)$$

and
$$\hat{k}_i^T(k+1) = \hat{k}_i^T(k) + \{u_i(k+1) - \hat{k}_i^T(k)y_p(k+1)\}$$
$$.y_p^T(k+1)R(k+1) \qquad (22)$$

where $k_i^T = (k_{i1} \ k_{i2} \ k_{i3} \ k_{i4})$ are the rows of K. Equations (21) and (22) may be used in an implicit self-tuning scheme, where the rows of K are estimated directly from the measurements u_a and y_p.

4.2 Combined AUR/FIR Scheme

As in the AUR identification, it is required only to estimate a parameterised mill matrix A (given in (9)) for an explicit scheme or for an implicit scheme, a controller matrix N (given from (6)). Since it is required to estimate a larger matrix, extra measurements are required, and are the FIR actuator positions. The equation upon which identification is to be performed is given as:

$$y_p = (PG_aP^T \ PG_i) u \qquad (23)$$

where $u = g(s)u'$ and $u' = \begin{bmatrix} Pu_a \\ u_i \end{bmatrix}$

A recursive estimate for the rows of A is easily obtained by following the procedure in 4.1. N may then be calculated via (8) giving explicit self-tuning control. Equation (23) may be rearranged to give:

$$u = N y_p \qquad (24)$$

whereupon the rows of N may be identified recursively, giving implicit self-tuning control. However, a matrix N calculated by this means will not be unique, since (24) describes a set of six equations, only four of which are linearly independent. If a right inverse matrix of a specific form is required, (e.g. in (8)), then an explicit scheme must be used.

5. NONLINEAR ACTUATOR EFFECTS

Two effects, due to the nonlinear nature of the actuators, are considered. The first concerns the identity of the estimated matrix and the second examines the beneficial effect of corrupting the sinusoidal shapemeter noise which propagates around the loop.

5.1 Identity of Estimated Matrix

In this section, it will be demonstrated that the matrix identified in the AUR case is not, in fact, PG_aP^T. The discrepancy is due to the nonlinear nature of the actuators since, for a linear actuator set, exact identification is achieved. A similar problem exists with the combined AUR/FIR scheme, but since no quantitative results are presented, the AUR case will be taken as the simplest example. Due to the dead-zone and backlash contained in the actuator loops (see Fig.3), the output vector will never equal the input, even in steady-state. The offset or difference will depend not only on the input but also the input history, since backlash contains memory. From Fig.1 it is seen that β contains only up to fourth order components, since α is of dimension 4. However, due to the actuator offset, the same cannot be said of u_a". Components are therefore produced in γ (and hence in y_p) that are not represented in u_a', since $u' = Pu_a$". The relationship between γ and u_a' is not due only to G_a and P ($\gamma = G_aP^Tu_a'$ for linear actuators), hence estimation of G_x using measurements of y_p and u_a' is impossible. The estimation error due to this phenomenon is not great and adequate control will be shown to be achieved with that matrix which is estimated. A more complete study of this effect, along with some numerical results, is given in (6).

5.2 Signal Corruption

Since the actuator outputs and inputs are rarely (if ever) equal, any signal passed through the actuators will be corrupted. This corruption becomes more pronounces for signals with an amplitude comparable to the magnitude of the actuator backlash and dead-zone. This, while in general an undesireable effect, prevents correlation between the shapemeter noise on the output and that which has propagated around the loop providing the identification signal. The amplitude of the shapemeter noise is about $1.2 \ n/mm^2$ (shape units).

6. LOW FREQUENCY DISTURBANCE REMOVAL

The incoming strip shape disturbance profile enters the mill between the input and output measurement points which are used for identification. Since this disturbance is essentially low frequency or d.c. in nature, biased estimates will result if its effect is not removed from y_p. An averaging process may be used on y_p to calculate (and remove) the low frequency disturbance signal. However, since that signal which is removed from y_p may contain components due to $u_a{}''$, an identical averaging process and subtraction must be applied to $u_a{}''$. A moving average S_n for the sequence x_n may be calculated as:

$$S_n = (1 - \rho) \sum_{r=0}^{\infty} \rho^r x_{n-r}$$

or recursively as:

$$S_{n+1} = \rho S_n + (1 - \rho) x_{n+1} \qquad (25)$$

where ρ is a weighting factor < 1 and gives exponential weighting over the sequence x_n. N is the number of points over which the averaging is performed, where $N = 1/(1 - \rho)$. It may be noted that (25) is equivalent in form to a discrete-time low pass filter, where

$$\rho = e^{-\Delta t/\tau} \qquad (26)$$

Δt being the discretisation interval and $1/\tau$ the corner frequency. An appropriate choice of ρ for the current application is 0.0091, giving a cut-off of 25.26 Hz.

7. PERFORMANCE

Results are presented for both AUR and combined AUR/FIR schemes for the implicit case (controller matrices identified directly).

7.1 As-U-Roll Control

To assess the quality of the controller estimates, a simulation run was performed for a medium speed plant where the most recent controller parameters were transferred directly to the controller. The identity matrix was used as an initial estimate for K and the error covariance matrix initialised at $10^5 I_4$. The target shape profile was chosen to be flat. The output shape profile variations with time for this run are shown in Fig.4 and the variation in parameter estimates for row 1 of K shown in Fig.5. The estimated values after 5 seconds are:

$$\hat{K} = \begin{bmatrix} 0.0633 & -0.0176 & 0.0408 & -0.1044 \\ 0.0325 & 0.1750 & 0.0624 & 0.5144 \\ 0.0132 & 0.0465 & 0.2231 & 0.1227 \\ 0.0601 & 0.1259 & 0.1446 & 0.9137 \end{bmatrix} \qquad (27)$$

$(PG_a P^T)^{-1}$ for this run is given as:

$$G_x{}^{-1} = \begin{bmatrix} 0.0670 & -0.0129 & 0.0599 & -0.0799 \\ 0.0345 & 0.1773 & 0.0971 & 0.5730 \\ 0.0205 & 0.0540 & 0.2615 & 0.1816 \\ 0.0616 & 0.1265 & 0.1826 & 0.9813 \end{bmatrix} \qquad (28)$$

7.2 AUR/FIR Control

As in the previous case, a simulation run was done to assess the performance of the implicit self-tuning controller. The starting value for each of the parameter estimates for this case was set at 0.5, with the error covariance matrix remaining at $10^5 I_4$. The output shape profile variations with time for this run are shown in Fig.6 with the variation in parameter estimates for row 6 of N (as an example) given in Fig.7. A measure of the quality of the right inverse obtained may be had by calculating the product $\hat{A}\hat{N}$ (which should equal I_4). Using the steady-state parameter values, this product has the values:

$$\hat{A}\hat{N} = \begin{bmatrix} 1.052 & -0.202 & -0.153 & 0.207 \\ 0.045 & 0.828 & -0.121 & 0.194 \\ -0.059 & 0.225 & 1.118 & -0.135 \\ -0.012 & 0.052 & 0.039 & 0.954 \end{bmatrix} \qquad (29)$$

8. EFFECT OF AN INACCURATE DYNAMIC MODEL

In the analysis presented so far, it has been assumed that the dynamic transfer function between roll-gap and measured shape profile (g(s)) is known to a reasonable degree of accuracy. However, since no conclusive tests regarding the validation (or otherwise) of the dynamic model have been performed (2), it is important to examine the effect of an inaccurate dynamic model on the identification scheme. To this end, a simulation run was performed where it was assumed (for estimation purposes) that g(s) consisted of:

$$g(s) = \frac{e^{-\tau_1 s}}{(1 + \tau_3 s)} \qquad (30)$$

The g(s) used in the mill simulation was as given in section 2. An error, therefore, in the order of g(s) is introduced. The simulation run was performed for a medium speed plant utilising both AUR's and FIR's as control devices. The output shape profile variations with time, for an implicit scheme, are shown in Fig.8. The parameter estimate variations for row 6 of N are given in Fig.9. The product $\hat{A}\hat{N}$ for this case is calculated as:

$$\hat{A}\hat{N} = \begin{bmatrix} 0.971 & 0.009 & -0.067 & -0.776 \\ -0.760 & 0.612 & 0.891 & -1.152 \\ -0.065 & -0.166 & 0.835 & -0.399 \\ 0.219 & 0.140 & -0.222 & 1.204 \end{bmatrix} \qquad (31)$$

9. DISCUSSION OF RESULTS

From Figs.5 and 8 it is seen that the estimates converge within about 4 seconds (the period of inactivity at the start is due to the time delay in the system). This is consistant with the shape profile variations of Figs 5 and 7, since good control is achieved after

the initial convergence period. The final values of the estimates for the AUR case are seen to be quite close to the values in G_x^{-1}. However, they cannot equal these values exactly due to the nonlinear effects of the actuators. For the same reason, the final values of the estimates for the AUR/FIR case cannot form an exact right inverse of A. However, a close approximation (as seen from (30)) is obtained. It may be noted that poor initial estimates were used for both K and N were used. In practice, better initial estimates will be available through the use of the static model, which will reduce convergence time and provide better initial control. The shape control for the case of g(s) mismatched (shown in Fig.8) is seen to be poor for a large portion of the simulation, but when the parameter estimates do converge, (after about 12 seconds) adequate control is achieved. The quality of the right inverse for this case is not as good as that for the matched case, since large off-diagonal elements appear in the product $A\hat{N}$ in (31). The poor initial control may be attributed partly to the poor initial estimates and may be improved by limiting the control inputs during the initial convergence period. Alternatively, a cost could be imposed on actuator movements from known 'safe' positions during the initial convergence period.

10. CONCLUSIONS

In the AUR/FIR scheme, some design freedom exists (in the choice of N), but exploitation of this freedom requires an explicit control law. The propagation of the shapemeter noise around the loop provides the identification signal, but may cause excessive wear on the actuator hydraulics. If this is found to be a problem, the shapemeter noise could be eliminated by the addition of some dead-zone or extra filtering on the shapemeter output. A PRBS could then be injected on the actuator inputs during startup (for initial parameter estimation) and at intervals triggered by large actuator movements (indicating a change in operating point). The duration of this PRBS need only be about 4 secs., since the parameters, in general, converge quite quickley. It has been shown that even when the model of g(s) is in error, reasonable parameter estimates are achieved (though convergence is slow). If it is found that the model is grossly in error, some identification tests

may be performed on the strip and shapemeter dynamics. Since g(s) is schedule independent, only one identification test for each mill speed may be performed.

REFERENCES

(1) G.W.D.M. Gunawardene, "Static Model Development For The Sendzimir Cold Rolling Mill", Ph.D. Thesis, Sheffield City Ploytechnic, 1982.
(2) K. Dutton,"An Investigation Into The Design and Performance of a Shape Control System For a Sendzimir Mill", Ph.D Thesis, Sheffield City Polytechnic, 1983.
(3) M.J. Grimble and J. Fotakis,"The Design of Shape Control Systems for Sendzimir Mills" IEEE Trans. Auto. Con., AC-27, pp 656-666, 1982.
(4) J.V. Ringwood and M.J. Grimble,"An Optimal Output Feedback Solution to The Strip Shape Multivariable Control Problem", Proc. IASTED Symp. on Applied Control and Identification , ACI 83, Copenhagen, 1984.
(5) J.V. Ringwood, D.H. Owens and M.J. Grimble "Feedback Design of a Canonical Multivariable System With Application to Shape Control in Sendzimir Mills", submitted Automatica 1984.
(6) J.V. Ringwood,"The Design of Shape Control Systems for a Sendzimir Mill", Ph.D. Thesis, University of Strathclyde, 1984.
(7) J.V. Ringwood, "Representation of a Class of Nonlinear System as a Time Varying Linear System of First Order", Research Report ICU/43/1984, Industrial Control Unit, University of Strathclyde, 1984.
(8) B. Noble, "Applied Linear Algebra", Prentice-Hall Inc., New Jersey, 1969.
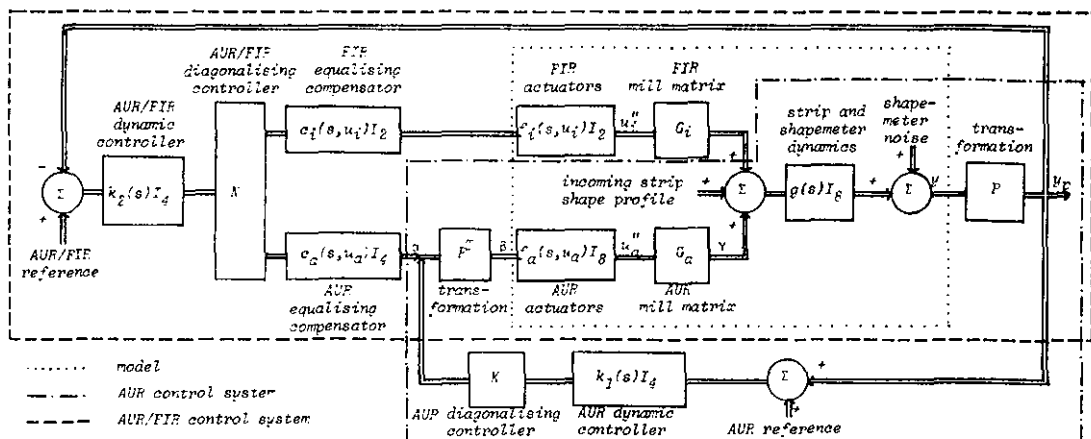(9) L. Ljung and T. Soderstrom,"Theory and Practice of Recursive Identification", MIT Press, Cambirge, Mass., 1983.

Figure 1: System block diagram showing AUR and AUR/FIR control structures
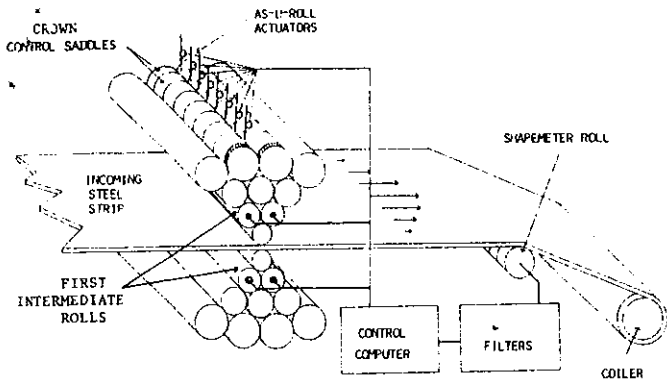
Figure 2 : Physical layout of Sendzimir mill

Figure 3: Actuator block diagram
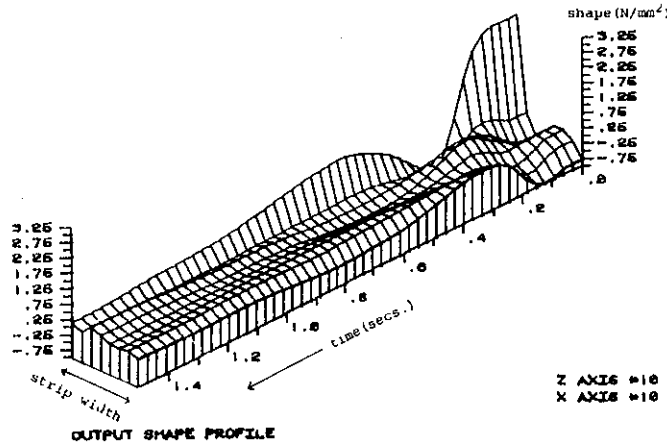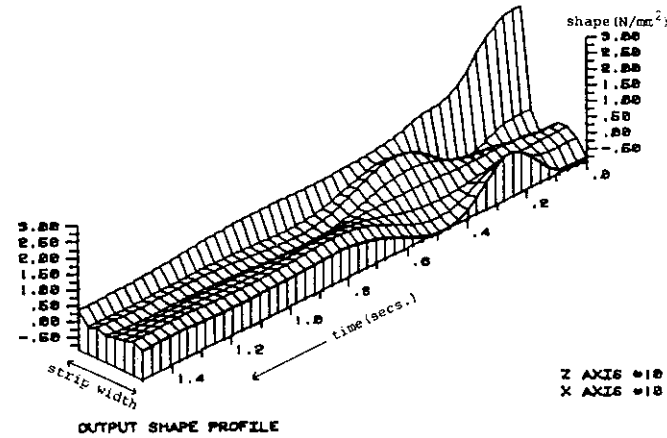

OUTPUT SHAPE PROFILE

Figure 4: Shape profile variations for AUR control

D-K(1,1)   -K(1,2)

D-K(1,3)   -K(1,4)
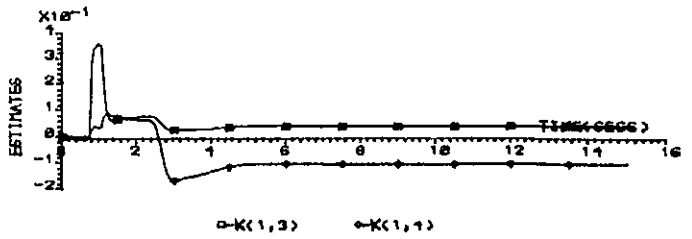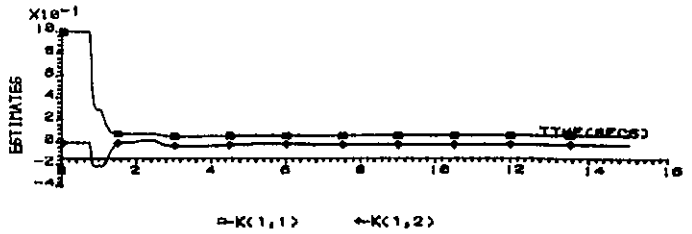
Figure 5: Parameter variations for row 1 of K

OUTPUT SHAPE PROFILE

Figure 6: Shape profile variations for AUR/FIR control

D-N(6,1)   -N(6,2)

D-N(6,3)   -N(6,4)
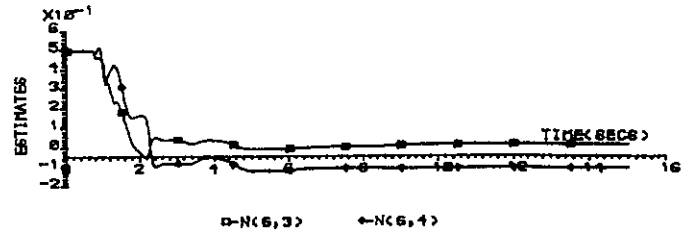
Figure 7 : Parameter variations for row 6 of N

OUTPUT SHAPE PROFILE

Figure 8 : Shape variations for mismatched g(s) using AUR/FIR control

D-N(6,1)   -N(6,2)

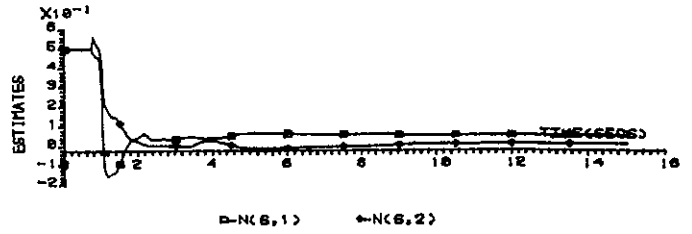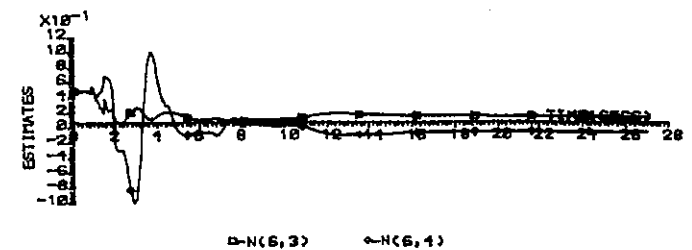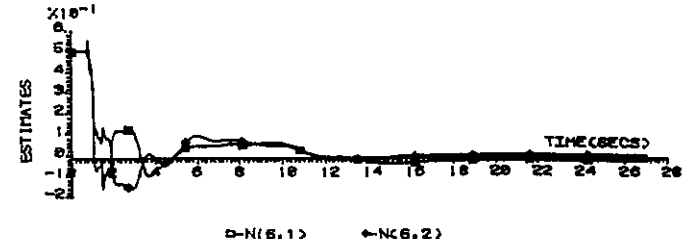D-N(6,3)   -N(6,4)

Figure 9: Parameter variations for row 6 of N for mismatched g(s)